

Effects of Dip-coating Processing Parameters on the Functional Performances of $\text{Ti}_3\text{C}_2\text{T}_x$ MXene-silk Yarns

Sirui Yao, Chen Meng, Qinghong Huang, Zekun Liu, Henry Yi Li*

University of Manchester, Sackville Street Building, Manchester, M1 3BB, United Kingdom

Abstract

Mxenes, as a new group of two-dimensional materials in form of transition metal carbides, carbonitrides and/or nitrides, have been playing an important role in the wearable smart electronic field. Due to their abundance surface functional groups, Mxenes have showed their superior dispersions in various solvents which is beneficial to simplify the fabrication process of textile-based electronics while their electrical performance guaranteed. In this work, we report a novel fine silk yarn dip-coated in an aqueous solution of $\text{Ti}_3\text{C}_2\text{T}_x$ MXene to obtain low electrical resistance (~ 25.6 Ohms/cm). Yarns structures and morphologies were observed by transmission and scanning electron microscopy (TEM & SEM) together with energy dispersive spectroscopy (EDS). Besides, Fourier transform infrared (FTIR) and Raman spectroscopy, and X-ray diffraction (XRD) analysis were carried out to reveal the chemical compositions. By controlling two coating parameters as design of experiments (DoE) factors, we found both solution concentration and soaking time had significant effects on yarn performances. The mechanical performance of yarn fabricated under the optimised coating condition was evaluated by means of tensile testing, resulting in a significant 23% increase in breaking strength (~ 107 MPa). In responding to tensile deformation, the dip-coated yarn also performed a linear variation in resistance, which indicated its capability in sensing applications.

Keywords: MXenes; Electrically Conductive Yarns; Dip-coating; DoE; Yarn Tensile Strength

1 Introduction

It has already been over a decade since the two-dimensional (2D) material $\text{Ti}_3\text{C}_2\text{T}_x$ was found as the first MXene [1] and followed by a rapid develop of the whole transition metal carbides, carbonitrides and/or nitrides family. From the chemical formula, Ti refers to the early transition metal titanium, C represents carbides, and T stands for surface termination functional groups involving hydroxyl (-OH), oxygen (-O) and fluorine (-F) which are beneficial to the hydrophilic nature of $\text{Ti}_3\text{C}_2\text{T}_x$ [2, 3]. $\text{Ti}_3\text{C}_2\text{T}_x$ MXene started to be very appealing to the wearable smart textile field because of its promising high electrical conductivity inherited from transition metal

*Corresponding author.

Email addresses: sirui.yao@postgrad.manchester.ac.uk (Sirui Yao), henry.yili@manchester.ac.uk (Henry Yi Li).

[4], the reported applications include but not limited to energy storage [5, 6], different types of sensors [7-9] and electromagnetic interference (EMI) shield [10, 11].

However, new findings pointed out one major issue would affect the long-term usage of MXene is degradation caused by oxidation in aqueous solution [12, 13]. Thus, the method to fabricate MXene with textile substrate can be critically complicated. As one of the most common used coating techniques for textiles, dip coating can be simply carried out regardless of production scales and keep the cost low while provide an uniform coating on cylindrical substrates efficiently [14]. Considering silk, as one of nature fibres, is also well known for its rich surface functional groups [15] which may lead to an efficient integrating with MXene, and therefore avoiding the degradation.

Herein, a cost-effective dip coating process was used in this work to fabricate a conductive silk yarn in order to shorten the producing time and additionally stabilised the MXene. Also, the impacts of the coating process parameters on yarns performance were studied in Minitab via a two-factor two-level method. The dip-coating process was then optimised with the best combination of settings. The as-made silk will then be tested for its mechanical and electrical behaviours. A relevant pilot study was reported in Textile Bioengineering and Informatics Society, 2022 [16].

2 Methodology

2.1 Materials

The two-ply 2/60 Nm Italian spun silk yarn was used as the substrate yarn for the dip-coating process in this work and was supplied by Uppingham Yarns, UK. The delaminated $\text{Ti}_3\text{C}_2\text{T}_x$ MXene powders was purchased from Nanoplexus Ltd.

2.2 Design of Experiments (DoE)

Considering the existed two parameters in the dip-coating process, one was the concentration of prepared coating solution, and another was the time duration of yarns soaked in the solution, a two-factor two-level DoE was used to figure out if these coating variables would affect the mechanical and electrical performance of coated yarn. The solutions were prepared in 10 mg/mL as low concentration and 15 mg/mL as high concentration, respectively, while the soaking duration was controlled in three minutes and five minutes, as shown in Table 1. The sample groups under different coating conditions were marked as 10-3 (10 mg/mL; 3 min), 10-5 (10 mg/mL; 5 min), 15-3 (15 mg/mL; 3 min) and 15-5 (15 mg/mL; 5 min). In each group, three specimens were prepared with 8 times repeated coating and tested for their electrical resistance. The results were analysed by using Minitab DoE software to identify the key processing parameters that have effects on the electrical resistance, and the best processing setup to achieve highest electrical conductivity. The details of DoE design settings in Minitab are as shown in Table 2.

Based on the results of the first experiment, the best experiment set-up was selected to confirm the results with a number of repeating dip-coating processes from one to eight times for understanding the effects of morphology and chemical composition distribution during coating on mechanical and electrical properties of the yarns.

Table 1: Two-factor two-level DoE for dip-coating process

Factors	Levels
A-Solution Concentration	10 mg/mL, 15 mg/mL
B-Soaking Duration	3 minutes, 5 minutes

Table 2: DoE Design Summary

Factors	2	Base Design	2, 4
Runs	12	Replicates	3
Blocks	1	Centre pts (total)	0

2.3 Fabrication of MXene-coated Silk Yarn

From the schematic illustration shown in Figure 1(a), 700 mg and 1,125 mg $\text{Ti}_3\text{C}_2\text{T}_x$ MXene powders were fully dispersed in 70 mL deionised (DI) water by using 500 rpm magnetically stirring for 2-hour. Thus, MXene aqueous solution at 10 mg/mL and 15 mg/mL concentrations were obtained, respectively. Two bundles of commercial silk yarns were soaked in as-prepared MXene-aqueous solution for three minutes when the rest two bundles were immersed in for 5 minutes, as designed in last subsection. The coating processes were repeated for eight times, and for every single time yarns were blow-dried to eventually obtain dip-coated MXene-silk yarns. All the procedures were done at room temperature.

2.4 Characterisation

To observe the morphology and microstructures of $\text{Ti}_3\text{C}_2\text{T}_x$ MXene flakes and those of yarns before and after dip-coating, a transmission electron microscope (TEM, FEI Tecnai 20, 200 kV) and a scanning electron microscope (SEM, FEI Quanta 250, 15 kV) were used. A small volume of prepared aqueous solution of $\text{Ti}_3\text{C}_2\text{T}_x$ MXene was further diluted with DI water, and the resulting solution was dropped on 400-mesh copper grids (SPI) for TEM operation. During the SEM, an energy dispersive spectroscopy (EDS, Oxford with AZtec software) was carried out at the same time for the further elemental quantitative analysis. The thickness of the MXene flakes was measured via atomic force microscopy (AFM, Bruker Multimode 8). Fourier transform infrared spectroscopy (FTIR, Thermo Fisher Nicolet 5700) was utilised to investigate the chemical states of not only $\text{Ti}_3\text{C}_2\text{T}_x$ MXene powder, but also pristine and dip-coated silk yarns. In addition, Raman spectra (Horiba LabRAM, 488 nm) and X-ray diffraction (XRD, PANalytical X'Pert Pro) patterns were retrieved with scanning ranges of 100–2000 cm^{-1} and 10–80°, respectively, to further identify the chemical compositions.

2.5 Functional Performance of MXene-coated Silk Yarn

The yarns mechanical behaviour before and after dip-coating were investigated at room temperature via tensile testing machine (Instron 3344 with 1 kN load cell). Three specimens were selected from original and treated silk yarns respectively. Each specimen was tested under a stretching

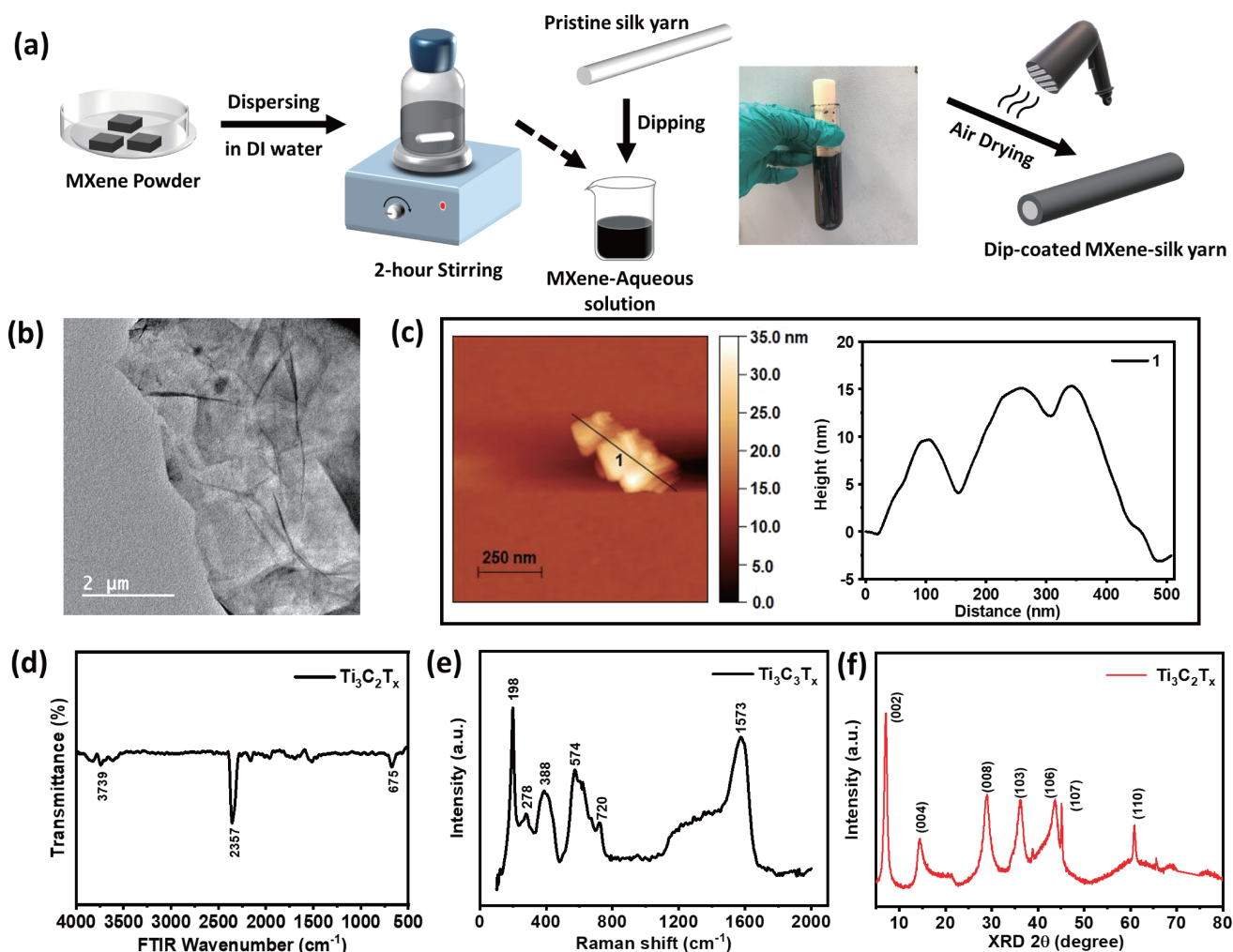


Fig. 1: (a) Illustration of MXene-Aqueous solution preparation and dip-coated MXene-silk yarn fabrication. Structural and chemical characterisation of multilayer Ti₃C₂T_x MXene: (b) TEM image; (c) AFM image with height measurement along the Line 1; and (d) FTIR, (e) Raman and (f) XRD spectra

rate of 0.5 mm/second with the fixed gauge length of 50 mm until it ruptured. Meanwhile, the change of yarn electrical resistance was tracked and recorded by a multimeter (Keithley 2000).

2.6 Statistical Analysis

The linear electrical resistance results of coated-yarns and EDX quantitative analysing results of chemical elements distribution on yarns surfaces and cross-sections were all plotted in terms of mean ± standard deviation via Origin 2021b. Within this software, the one-way ANOVA test was proceeded to determine the intergroup differences in either yarn linear electrical resistance after multiple times repeated coating processes or yarns mechanical properties before and after being dip-coated. In the results, the p-value more than 0.05 was expressed as NS which means no significant difference, and for those p-values less than 0.05, and 0.001 were flagged as one star (*) and triple stars (***) respectively, both of which represent significant difference. The impact of coating solution concentration and soaking duration on yarn electrical performance was analysed in statistical software Minitab 19. Stepwise regression tool was used within the same software to

find out the correlation among all variables and therefore reveal the effect of applying MXene on yarn electric performance.

3 Results

3.1 $\text{Ti}_3\text{C}_2\text{T}_x$ MXene Flakes Characterisation

3.1.1 Morphology and Structure

$\text{Ti}_3\text{C}_2\text{T}_x$ MXene flakes' multi-layer structure was revealed by the TEM result in Figure 1(b), which can also be confirmed by its AFM image and the height profile measured across the particle in Figure 1(c). The $\text{Ti}_3\text{C}_2\text{T}_x$ particle had a size of approximately 500 nm and an average thickness of about 15 nm.

3.1.2 Chemical Composition

FTIR, Raman and XRD analysis were conducted to better understand the surface functional groups $\text{Ti}_3\text{C}_2\text{T}_x$ MXene has and figure out how they interact with the textile substrates during dip-coating. As for FTIR displayed in Figure 1(d), the visualised broad peak appeared at 3740 cm^{-1} which confirmed the presence of -OH groups [17], and therefore, $\text{Ti}_3\text{C}_2\text{T}_x$ MXene was hydrophilic and humidity sensitive [9, 18]. The sharp intensity absorption at 2357 cm^{-1} , followed by the existed lower intensity peak at frequencies range of $800\text{-}600\text{ cm}^{-1}$ possibly indicated the carbon triple bond $\text{C}\equiv\text{C}$ [19].

Besides, Figure 1(e) demonstrated the Raman spectrum of $\text{Ti}_3\text{C}_2\text{T}_x$ MXene flakes. The peaks located at around $198, 278, 574$ and 720 cm^{-1} were known as key features of $\text{Ti}_3\text{C}_2\text{T}_x$ MXene, associated with in-plane Ti-C vibrations, solely carbon vibrations and C-C vibrations, respectively [2, 20, 21]. The 1573 cm^{-1} band was ascribed to D and G peak of graphitic carbon as it was observed within the range of $1000\text{-}1800\text{ cm}^{-1}$ [22, 23].

Sharp diffraction peaks were obtained from XRD testing on MXene (see in Figure 1(f), with the most intense one occurred at the $2\theta = 7.1^\circ$ which was related to (002) [9, 11], followed by other three detected at $14.5^\circ, 29.0^\circ$ and 60.9° indicating (004) [24], (008) and (110) [22] planes respectively.

3.2 Pristine and Dip-coated MXene-silk Yarns Morphology Analysis

From Figure 2(a), the first column of images, pristine silk yarn showed the fine and smooth yarn surface in its SEM image with visible distribution of chemical elements carbon (C), nitrogen (N), and oxygen (O) from EDS mapping images. On the surfaces of all four groups coated yarns after eight times repeated coating processes, MXene flakes wrapped around yarns tightly and evenly, according to the SEM images of yarns shown in Figure 2(b)-2(e). Comparing to the pristine yarn, even though the applied MXene turned the smooth yarn surface into relatively rough, but its presence did not affect the yarn fineness too much, no matter in which group. The EDS mapping results of coated yarns demonstrated the appearance of two more elements fluorine (F) and titanium (Ti), which indicated the successful deposition of MXene since they are

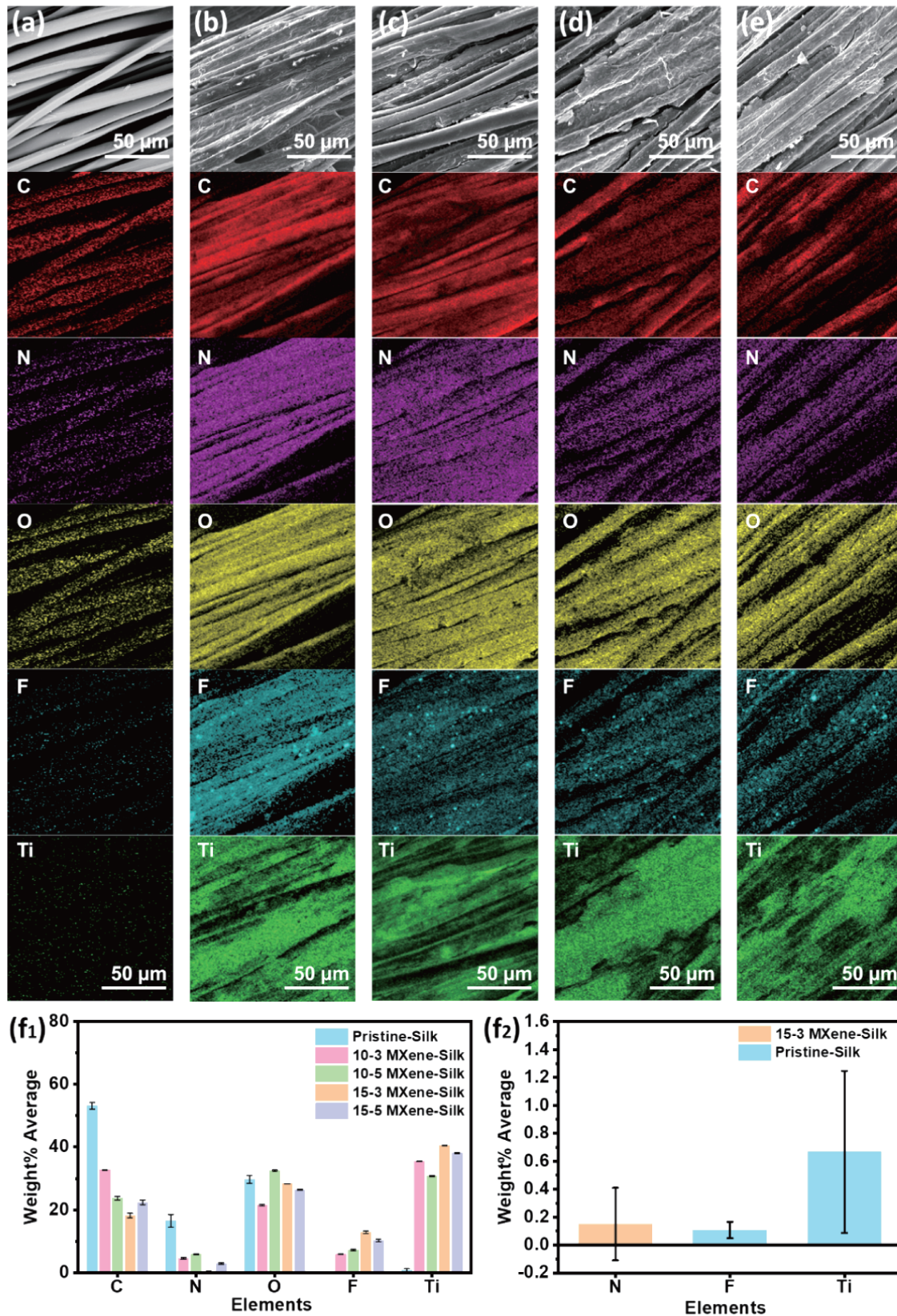


Fig. 2: Morphological and chemical characterisation: SEM images and EDS element maps of MXene-coated yarns after dip-coating for 8 times with different coating parameters: (a) pristine, (b) 10-3, (c) 10-5, (d) 15-3 and (e) 15-5; (f₁) Quantitative analysis of basic elements distribution on the surface yarns with (f₂) more details

two other main elements apart from C, N, and O [2, 25]. Additionally, higher elemental signals were detected from the coated yarn, resulting in distinctly more intense colours. Moreover, the quantitative analysis in Figure 2(f_1) & (f_2) showed the overall proportion decrease of both elements C and N from 53.12 and 16.44 wt% as in pristine yarn to 32.67, 23.72, 18.16 and 22.42 wt% of C, and 4.47, 5.79, 0.15 and 2.85 wt% of N as in group 10-3, 10-5, 15-3 and 15-5 respectively. Conversely, the concentrations of elements F and Ti had significant increases from 0.11 and 0.67 wt% to 5.85, 7.19, 12.86 and 10.23 wt% of F, and 35.47, 30.78, 40.52 and 38.09 wt%, respectively in each group after coating.

3.3 Electrical Performance of Dip-coated Yarns

After repeating the dip-coating process for 8 times for each sample group, the final measurements of yarn electrical linear resistance were presented in Figure 3. Yarns coated with 10 mg/mL solution concentration and 3-minute soaking duration in each coating cycle resulted in the lowest resistance of ~ 25.6 ohms/cm, while those coated under the same solution concentration but 2 minutes longer soaking duration came out with ~ 45.06 ohms/cm as the highest among 4 groups. The impact effects of coating parameters on yarn electrical performance will be discussed with DOE factorial analysis details in the Section 4.

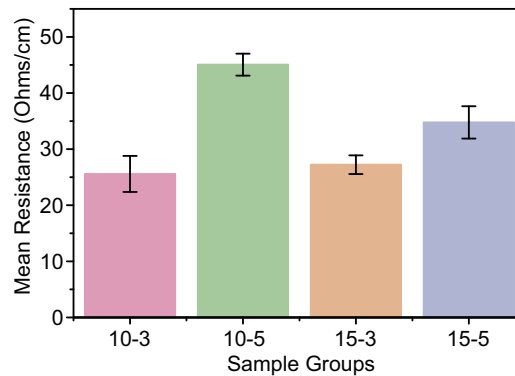


Fig. 3: Electrical resistance of four sample groups under different dip-coating setup

3.4 Pristine and 10-3 MXene-silk Yarn Comparison

Since the Group 10-3 of MXene-silk yarns has already shown the lowest electrical resistance, this combination of dip-coating processing parameters could be the best choice to get the ideal conductive yarn. Therefore, a yarn specimen was randomly picked out from this sample group and compared with the pristine silk yarn regarding their differences in chemical composition and mechanical properties. Figure 4(a) is the SEM image of the selected yarn after coating.

The FTIR spectrum for pristine yarn in Figure 4(b) exhibited particular absorption peaks at 1622 cm^{-1} , 1512 cm^{-1} , 1223 cm^{-1} , and 690 cm^{-1} , which corresponded to the presence of amide I, II, III, and V bands in silk, respectively [25–27]. Another strong peak of hydrogen bond (-NH) presented at 3271 cm^{-1} [28], which was almost invisible in the spectrum of dip-coated yarn. There were few more noticeable decreases in intensity of peaks with slightly shifted positions into 1648 cm^{-1} (amide I) and 1517 cm^{-1} (amide II). In addition, two peaks were detected at 3271 cm^{-1} and

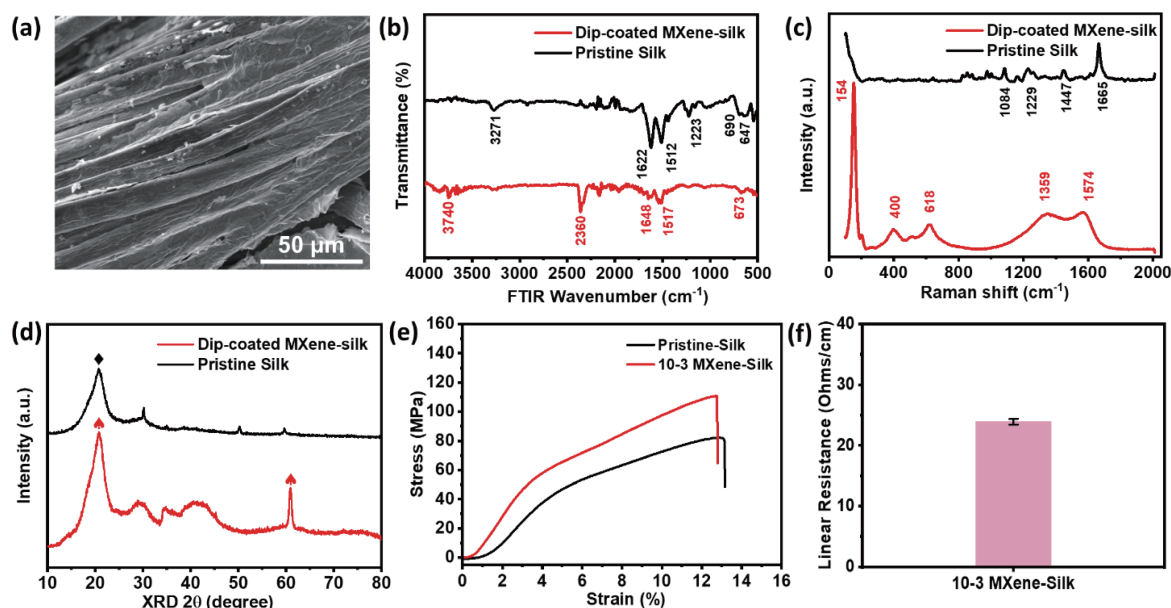


Fig. 4: (a) SEM image showed morphology of one MXene-coated yarn specimen from 10-3 group after 8 times coating; Chemical and structural characterizations comparisons of pristine and this coated yarn: (b) FTIR, (c) Raman and (d) XRD spectra; (e) Strain-stress curve under tensile test, and (f) electrical resistance

2360 cm^{-1} which were -OH and $\text{C}\equiv\text{C}$ as mentioned in MXene flakes characterisation. Although the previous EDS reports stated the presence of F, the absorption peak of C-F was not as obvious as other bonds. The varied peak intensities, plus peak disappearance or appearance illustrated there were chemical bonds changed between $\text{Ti}_3\text{C}_2\text{T}_x$ MXene and silk during dip-coating process.

Raman spectra in Figure 4(c) were consistent with the same finding. The bands at 1084 , 1447 and 1665 cm^{-1} were assigned to the β -sheet structure for pristine silk yarn [29, 30], while the peaks with high intensity at 1229 and 1665 cm^{-1} related to amide III and I [31, 32]. These peaks clearly decreased after MXene applied onto the yarn. Instead, the coated yarn exhibited comparable peaks at 154400 and 618 cm^{-1} signifying the presence of Ti-C and C-C vibrations as discussed in the previous MXene Raman analysis. Also, compared with the MXene Raman spectrum, the D and G bands of graphitic carbon at 1359 and 1574 cm^{-1} became more obvious.

Corresponding to the crystalline structure of silk II (β -sheet content), an intense peak appeared at $2\theta = 20.7^\circ$ in XRD spectra shown in Figure 4(d) [15, 33]. The $\text{Ti}_3\text{C}_2\text{T}_x$ MXene coating resulted in broadened peaks at 28.9° and 40.6° as amorphous signals [34], while maintaining the peaks at 20.8° and 60.9° (110) with high intensities.

The mechanical performance of coated yarns was demonstrated in term of strain-stress curves of yarn in Figure 4(e) with the data gathered from the yarn tensile tests. The strain and strength before fracture of untreated yarn were 13.0% and 82.1 MPa , respectively. The breaking elongation of treated yarns slightly decrease by 0.3% , while its breaking strength increased by 28.6 MPa , comparing to the original silk yarn. The electrical performance of as-coated yarn was measured by linear resistance and resulted in $\sim 24\text{ ohms/cm}$ as shown in Figure 4(f).

The cross-section of both yarns was also observed by SEM with EDS elements quantitative analysis. Images on the left corner of Figure 5(a) & (b) revealed single fibres in coated yarn retained a similar cross-section size compared to pristine yarn, except they had rougher outer

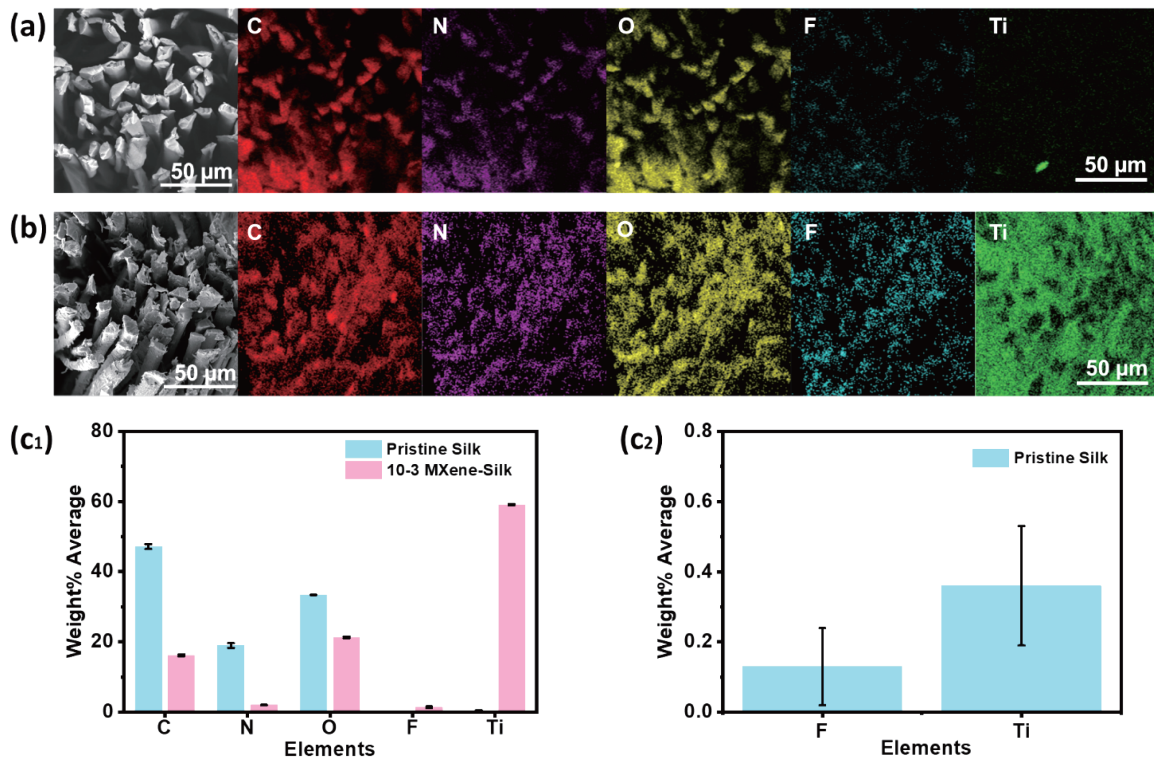


Fig. 5: Morphological and chemical characterisation: SEM images and EDS element maps of (a) pristine yarn cross-section and (b) 10-3 8 times MXene-coated silk yarn cross-section; (c₁) Quantitative analysis of basic elements distribution on cross-section of yarns with (c₂) more details for pristine yarn

edges. The same as EDS mapping results of yarn surfaces shown in previous subsection, those of yarn cross-sections presented higher colour intensities for each basic chemical elements after coating, especially for F and Ti. Additionally, the distribution of elements F and T also filled in the gaps among single fibres, which indicated the MXene deposition occurred not only on yarn surface but also cushioned the gaps. Comparing the elements quantitative results between two yarns (see in Figure 5(c₁) & (c₂)), the concentrations of C, N and O dropped from 47.16, 18.95 and 33.39 wt% into 16.19, 2.04 and 21.31 wt%, respectively, after coating. A slightly rise by 1.25 wt% occurred in the concentration of F, while a remarkable growth from 0.36 to 59.08 wt% of Ti content can be seen owing to the MXene presence.

4 Discussions

4.1 Impact of Coating Parameters on Electrical Performance

Considering two parameters were involved along the whole coating processes, it was worth determining if they could affect the electrical performance of as-made yarn, and therefore the dipping process can be optimised with the most ideal coating settings combination. By running the mean and standard deviation of yarn resistance measurements following factorial design in Minitab 19, the statistical results were pulled out in Figure 6(a)-(f).

From Figure 6(a), Group 10-3 provided the coated yarn with lowest electrical resistance. However, its confidence interval was the widest and was overlapped with Group 15-3 and Group 15-5

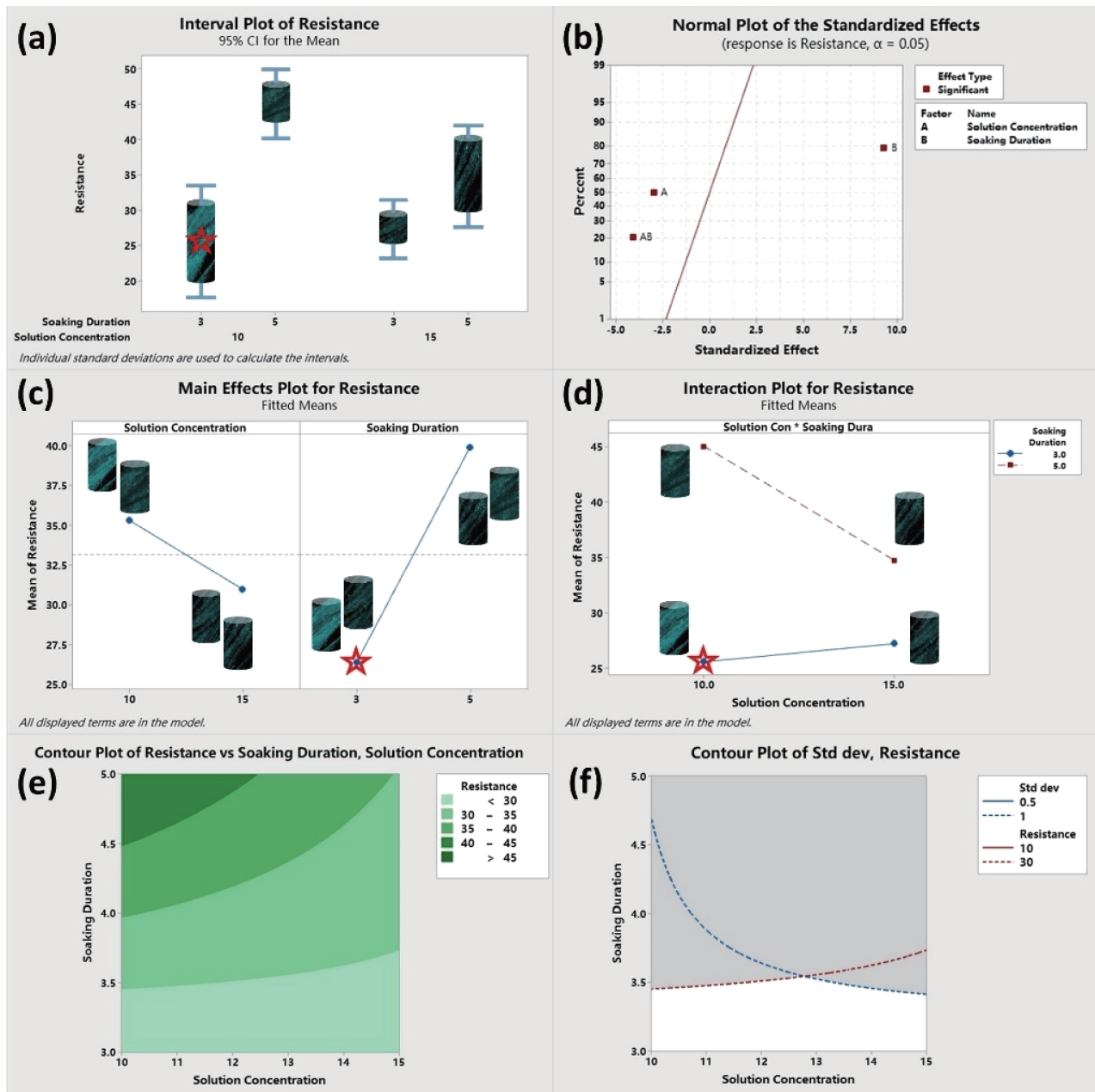


Fig. 6: Statistical results of dip-coating processing parameters effects on yarn electrical resistance. The legends representing each sample group were EDS maps of element F on yarn surface accordingly

but not overlapped with Group 10-5, which indicated the mean of the Group 10-3 was significantly different from Group 10-5 but might not be significantly different than the means of the other two groups. Both factors, solution concentration (A) and soaking duration (B), and their interaction AB were marked red in Figure 6(b), which meant they all had significant effects at 95% confident level. Additionally, soaking duration had larger effect on yarn resistance than solution concentration, and their interaction was strong with low corresponding p-value, as shown in Figure 6(c) & (d), respectively. Figure 6(e) & (f) were contour plots which demonstrated the shorter the soaking duration and the lower the solution concentration, the lower and more stable the yarn resistance. Therefore, the best combination of coating parameters was Group 10-3.

4.2 Mechanism Behind Effects

In order to understand the mechanism of the effects on dip-coated conductive yarns, a further statistical analysis was carried out, and the results of which were gathered in Figure 7. It detailedly determined whether those parameters of coating process also influenced the distribution results

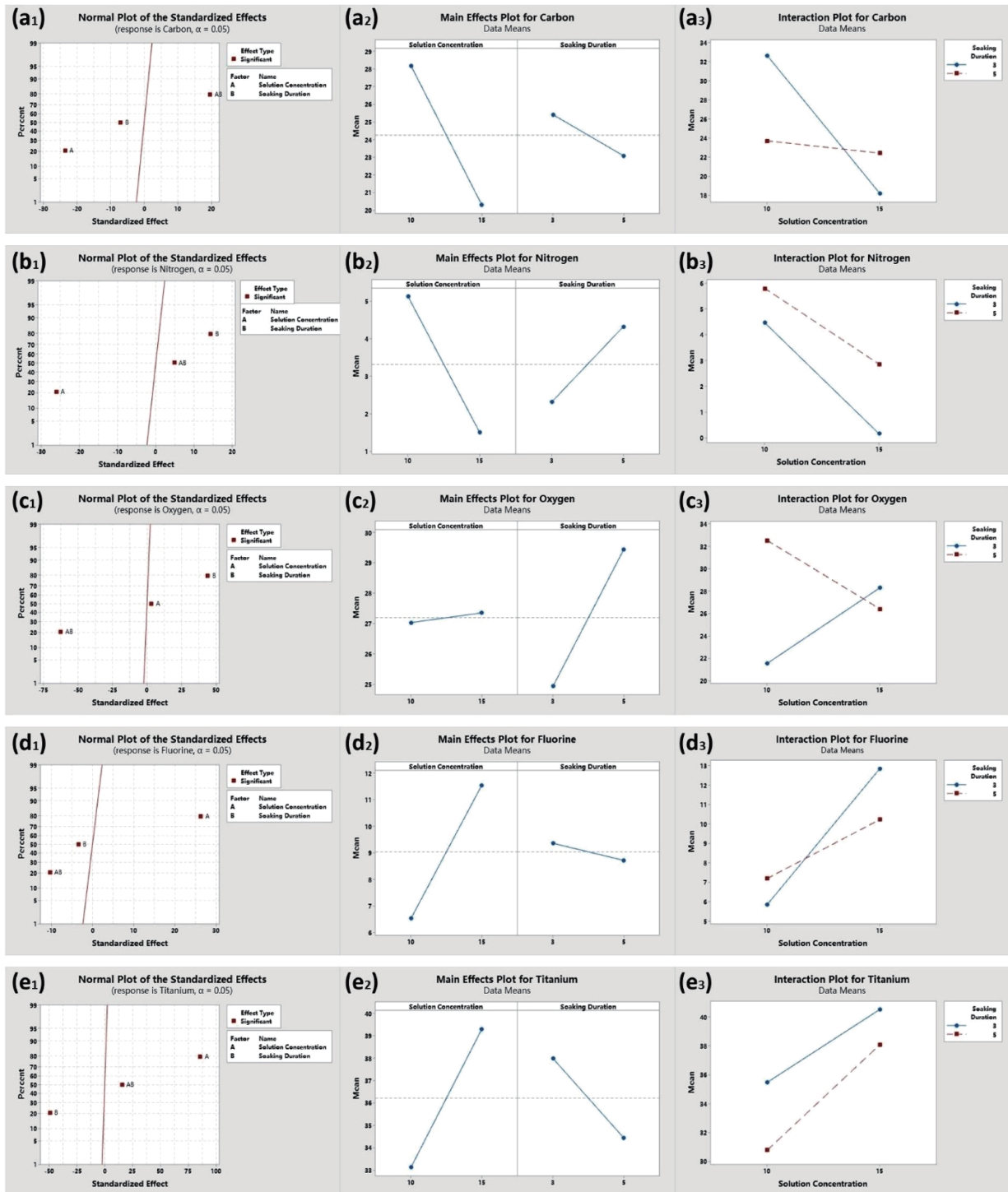


Fig. 7: Dip-coating process parameters effects on EDX quantitative analysis of yarns chemical elements: (a) carbon, (b) nitrogen, (c) oxygen, (d) fluorine, and (e) titanium

of chemical elements under EDS mapping technique. Moreover, correlation of yarn resistance and the corresponding elements distribution was studied within Group 10-3 regarding the repeated times of coating, since they were fabricated with the best coating setup combination.

4.2.1 Significant Factors

In general, solution concentration (A), soaking duration (B) and their interaction (AB) all significantly affected the mapping concentration of every element detected in coated yarn, but varied in magnitudes and directions, as shown in the first column of plots in Figure 7. For instance, in Figure 7(a₁), both A and B had statistically negative effects, yet the interaction AB resulted in a positive effect. In addition, A had AB changed the response much more than B did. As mentioned before, elements F and Ti were specifically existed in MXene. According to Figure 7 (d₁) & (e₁), A showed the most significant positive impact on both responses, and B retained negative effects. The interaction AB, on the other hand, decreased F concentration but increased Ti response when AB itself increased, and vice versa.

4.2.2 Main Effect

The middle column in Figure 7 presented the stronger impact of solution concentration on element concentrations than that of soaking time, except the response of element O as shown in Figure 7(c₂). In addition, higher solution concentration resulted in lower element concentrations of C and N, but higher concentrations for the rest of elements.

4.2.3 Interactions

Although all the plots in the last column of Figure 7 revealed the existence of interactions, the strength of interaction differed among elements being affected. The crossed lines shown in Figure 7(a₃), (c₃) & (d₃) represented more significant interactions between factors when discussed the effects on the concentrations of elements C, O and F, respectively, comparing to the relatively more parallel lines with the responses of N and Ti.

4.2.4 Repeated Coating Times Effect

Figure 8(a) showed the measured yarn linear resistance after repeating the coating process until the 8 times under the best coating settings. The resistance sharply fell between the first two coating processes, followed by another sudden drop from the second to the third group. It may be caused by the uneven coverage of MXene on the yarn surface. It kept resulting in statistically significant difference between adjacent groups in one-way ANOVA tests until it eventually came out with non-significant difference between the 7th and 8th times of coating. In another word, repeating coating process could improve the conductivity of as-made yarn, but it would no longer have a significant effect after 7th coating and reached the lowest linear resistance of ~ 25.6 ohm/cm at the 8th. This was the reason for all four groups of yarns with different coating parameters were coated repeatedly for 8 times.

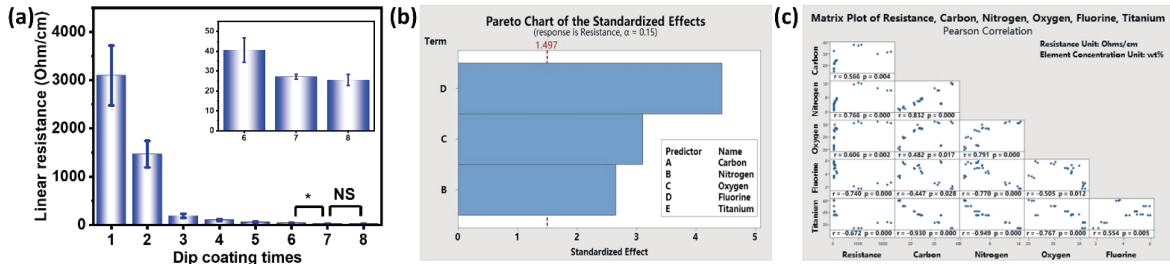


Fig. 8: (a) Linear resistance of Group 10-3 yarns after one to eight times repeated coating (insert: last three groups in smaller Y-axis scale); (b) Pareto Chart of chemical elements effects on 10-3 yarns linear resistances with different coating times and (c) correlations and p-values of these variables

4.2.5 Correlation of Yarn Electrical Resistance and Elements

Following the stepwise regression analysis, only the concentrations of elements N, O and F were statistically significant effects on yarn resistance among every coating cycle, as shown in Figure 8(b), among which F concentration was the strongest effect. In addition, considering elements F and Ti can only occur after accomplishing yarn coating process using MXene, the correlation matrix demonstrated that there was a moderate negative relationship between F concentration and yarn resistance, and Ti concentration and yarn resistance. This negative relationship indicated only when the MXene involved and led the F and Ti element concentrations increased, the yarn linear resistance after coating would decrease.

4.3 Mechanical Performance

According to Figure 9(a), the strain-stress curves obtained from the yarn tensile testing on pristine and MXene-coated yarn specimens shared similar trends. The initial 0-2.5% extension can be defined as a nonlinear region, because the fibre crimp normally exists in natural fibre yarn like silk [35, 36]. Beyond 2.5% extension, all curves presented a linear relationship between strain and stress until a sudden drop occurred when yarn ruptured eventually. By deeper investigations on their elongation at break and breaking strength (see in Figure 9(b)), the coated yarn exhibited a 23% in tensile strength with an average value of ~ 107 MPa, comparing to untreated yarn. This substantial enhancement can be attributed to the bridging effect of MXene flakes wrapped around the fibres [37] and chemical bonds generated between MXene and silk. The elongation at break

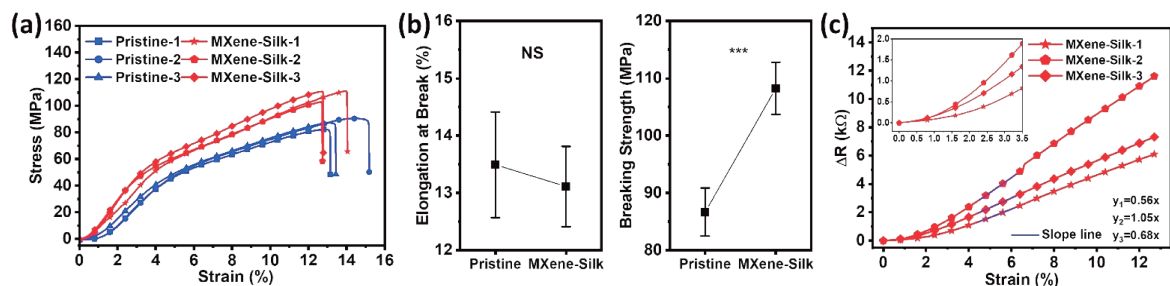


Fig. 9: Mechanical properties comparisons between pristine and coated yarns: (a) Stress-Strain curves; (b) Elongation at break and breaking strength; (c) Resistance variations of MXene-coated yarn during stretching

of coated yarn varied less than that of pristine yarn, although their mean breaking points were both fell at around 13.5%.

Figure 9(c) demonstrated the resistance change of each yarn specimen against varying strain within the ongoing tensile test. Apparently, the resultant resistance and tensile strain were highly linearly correlated during stretching, especially in the strain range of 2.5%-12.5%, which is highly compatible with yarn mechanical performance as illustrated above.

5 Conclusions

In this work, the dip-coating process was carried out following DoE with two different coating parameters to apply an aqueous solution of $Ti_3C_2T_x$ MXene on silk yarn and therefore to make a flexible conductive yarn. This low-cost but high-efficient method provided coated-yarn with a visible change in morphology from SEM images. The distribution of key elements of MXene including C, N, O, F, and Ti was observed from EDS mapping results which confirmed that MXene not only successfully covered the yarn surface but also filled in the gaps among fibres. All those shifted positions, varied intensities and appearance/disappearance of peaks revealed the changes in chemical bonds throughout the dip-coating process, which can be conducive to improve yarn mechanical property. Moreover, the statistical analysis showed both coating settings had significant effects on electrical properties of as-made yarns, especially soaking time. The best coating setup combination was 10 mg/mL solution concentration with 3 minutes soaking. The times of coating repetition also had impact on yarn resistance, and it achieved the best resistance of ~ 25.6 ohms/cm after eight times repeated processes. In fact, as-made yarn did perform better strength during the tensile tests despite it remained at similar breaking point. Additionally, it showed a linear variation of resistance corresponding to the applied deformation. The mechanical and electrical performance of dip-coated MXene-silk yarn may help pave the way for sensing applications in forms of yarn-based or further fabricated into fabric-based sensor.

References

- [1] Naguib, M., et al., Two-Dimensional Nanocrystals Produced by Exfoliation of Ti_3AlC_2 . 2011, 23(37): 4248-4253.
- [2] Sengupta, A., et al., Comparative Evaluation of MAX, MXene, NanoMAX and NanoMAX-derived-MXene for Microwave Absorption and Li ion Battery Anode Applications. *Nanoscale*, 2020, 12.
- [3] Naguib, M., et al., 25th anniversary article: MXenes: a new family of two-dimensional materials. *Adv Mater*, 2014, 26(7): 992-1005.
- [4] Hwu, H.H. and J.G. Chen, Surface Chemistry of Transition Metal Carbides. *Chemical Reviews*, 2005, 105(1): 185-212.
- [5] Yan, J., et al., Polypyrrole–MXene coated textile-based flexible energy storage device. *RSC Advances*, 2018, 8(69): 39742-39748.
- [6] Li, K., et al., 3D MXene Architectures for Efficient Energy Storage and Conversion. *Advanced Functional Materials*, 2020, 30(47): 2000842.
- [7] Li, T., et al., A flexible pressure sensor based on an MXene–textile network structure. *Journal of Materials Chemistry C*, 2019, 7(4): 1022-1027.

- [8] Sarika Pal, et al., Sensitivity Analysis of Surface Plasmon Resonance Biosensor Based on Heterostructure of 2D BlueP/MoS₂ and MXene, in *Layered 2D Advanced Materials and Their Allied Applications*. 2020, 103-129.
- [9] Haq, Y.-U., et al., Synthesis and characterization of 2D MXene: Device fabrication for humidity sensing. *Journal of Science: Advanced Materials and Devices*, 2022, 7(1): 100390.
- [10] Wang, Q.-W., et al., Multifunctional and Water-Resistant MXene-Decorated Polyester Textiles with Outstanding Electromagnetic Interference Shielding and Joule Heating Performances. *Advanced Functional Materials*, 2019, 29(7).
- [11] Zheng, X., et al., Breathable, durable and bark-shaped MXene/textiles for high-performance wearable pressure sensors, EMI shielding and heat physiotherapy. *Composites Part A: Applied Science and Manufacturing*, 2022, 152: 106700.
- [12] Wang, X., Z. Wang, and J. Qiu, Stabilizing MXene by Hydration Chemistry in Aqueous Solution. *Angewandte Chemie International Edition*, 2021, 60(51): 26587-26591.
- [13] Ding, Y., et al., Realizing ultra-stable Ti₃C₂-MXene in aqueous solution via surface grafting with ionomers. *Soft Matter*, 2021, 17(18): 4703-4706.
- [14] Joshi, M. and B. S. Butola, 14 - Application technologies for coating, lamination and finishing of technical textiles, in *Advances in the Dyeing and Finishing of Technical Textiles*, M.L. Gulrajani, Editor. 2013, Woodhead Publishing. 355-411.
- [15] JaramilloQuiceno, N. and A. RestrepoOsorio, Waterannealing treatment for edible silk fibroin coatings from fibrous waste. *Journal of Applied Polymer Science*, 2020, 137(13): 48505.
- [16] Yao, S., et al. A Pilot Study of Functional Performances of Dip-coated Ti₃C₂Tx MXene-silk Yarn. in *15th Textile Bioengineering and Informatics Symposium Proceedings, (TBIS 2022)*. 2022. Technical University of Liberec, Faculty of Textile Engineering: Textile Bioengineering and Informatics Society (TBIS).
- [17] Lee, E., et al., Room Temperature Gas Sensing of Two-Dimensional Titanium Carbide (MXene). *ACS Applied Materials & Interfaces*, 2017, 9(42): 37184-37190.
- [18] Hope, M. A., et al., NMR reveals the surface functionalisation of Ti₃C₂ MXene. *Physical Chemistry Chemical Physics*, 2016, 18(7): 5099-5102.
- [19] Nandiyanto, A.B.D., R. Oktiani, and R. Ragadhita, How to Read and Interpret FTIR Spectroscopy of Organic Material. *Indonesian Journal of Science & Technology*, 2019, 4(1): 22.
- [20] Mustakeem, M., et al., MXene-Coated Membranes for Autonomous Solar-Driven Desalination. *ACS Applied Materials & Interfaces*, 2022, 14(4): 5265-5274.
- [21] Presser, V., et al., First-order Raman scattering of the MAX phases: Ti₄AlN, Ti₂AlC_{0.5}N_{0.5}, Ti₂AlC, (Ti_{0.5}V_{0.5})₂AlC, V₂AlC, Ti₃AlC₂, and TiGeC₂. *Journal of Raman Spectroscopy*, 2012, 43(1): 168-172.
- [22] Iqbal, A. and N.M. Hamdan, Investigation and Optimization of Mxene Functionalized Mesoporous Titania Films as Efficient Photoelectrodes. *Materials*, 2021, 14(21): 6292.
- [23] Liu, F., et al., Preparation and methane adsorption of two-dimensional carbide Ti₂C. *Adsorption*, 2016, 22(7): 915-922.
- [24] Wang, H., et al., Surface modified MXene Ti₃C₂ multilayers by aryl diazonium salts leading to large-scale delamination. *Applied Surface Science*, 2016, 384: 287-293.
- [25] Asakura, T., et al., Conformational characterization of Bombyx mori silk fibroin in the solid state by high-frequency carbon-13 cross polarization-magic angle spinning NMR, x-ray diffraction, and infrared spectroscopy. *Macromolecules*, 1985, 18(10): 1841-1845.
- [26] Park, H.J., et al., Fabrication of microporous three-dimensional scaffolds from silk fibroin for tissue engineering. *Macromolecular Research*, 2014, 22(6): 592-599.

- [27] Kim, U.-J., et al., Structure and Properties of Silk Hydrogels. *Biomacromolecules*, 2004, 5(3): 786-792.
- [28] Zhang, R., et al., Sterilization of mycete attached on the unearthed silk fabrics by an atmospheric pressure plasma jet. *Chinese Physics B*, 2018, 27(5): 055207.
- [29] Zhang, Y.-Q., et al., Formation of silk fibroin nanoparticles in water-miscible organic solvent and their characterization. *Journal of Nanoparticle Research*, 2007, 9(5): 885-900.
- [30] Gasymov, O., et al., IR ellipsometry of silk fibroin films on Al nanoislands. *physica status solidi (c)*, 2015, 12.
- [31] Monti, P., et al., Raman spectroscopic studies of silk fibroin from *Bombyx mori*. *Journal of Raman Spectroscopy*, 1998, 29(4): 297-304.
- [32] Baranowska-Korczyn, A., et al., Silk Powder from Cocoons and Woven Fabric as a Potential Bio-Modifier. *Materials*, 2021, 14(22): 6919.
- [33] Gianak, O., et al., Silk Fibroin Nanoparticles for Drug Delivery: Effect of Bovine Serum Albumin and Magnetic Nanoparticles Addition on Drug Encapsulation and Release. *Separations*, 2018, 5(2): 25.
- [34] Xue, Q., et al., Photoluminescent Ti₃C₂ MXene Quantum Dots for Multicolor Cellular Imaging. *Advanced Materials*, 2017, 29(15): 1604847.
- [35] Wang, J., et al., Statistical modelling of tensile properties of natural fiber yarns considering probability distributions of fiber crimping and effective yarn elastic modulus. *Composites Science and Technology*, 2022, 218: 109142.
- [36] Belaadi, A., M. Bouchak, and H. Aouici, Mechanical properties of vegetal yarn: statistical approach. *Composites Part B: Engineering*, 2016, 106: 139-153.
- [37] Yang, Y., et al., Strain Sensors with a High Sensitivity and a Wide Sensing Range Based on a Ti₃C₂T_x (MXene) Nanoparticle–Nanosheet Hybrid Network. *Advanced Functional Materials*, 2019, 29(14): 1807882.